Bromelain Surface Modification Increases the Diffusion of Silica Nanoparticles in the Tumor Extracellular Matrix

Alessandro Parodi,[†,‡,⊗] Seth G. Haddix,[†,⊗] Nima Taghipour,[†] Shilpa Scaria,[†] Francesca Taraballi,[†,▽] Armando Cevenini,[†,§,⊥] Iman K. Yazdi,[†,∥] Claudia Corbo,[†,‡] Roberto Palomba,[†,‡] Sm Z. Khaled,[†] Jonathan O. Martinez,[†,#] Brandon S. Brown,[†,#] Lucas Isenhart,[†] and Ennio Tasciotti[†,*]

[†]Department of Nanomedicine, Houston Methodist Research Institute, Houston, Texas 77030, United States, [‡]Fondazione SDN IRCCS, Naples 80143, Italy, [§]Department of Molecular Medicine and Medical Biotechnology, University of Naples "Federico II", Naples 80131, Italy, [⊥]CEINGE-Biotecnologie Avanzate, s.c.a r.l., Naples 80145, Italy, [∥]Department of Biomedical Engineering, University of Houston, Houston, Texas 77204, United States, [#]The University of Texas Health Science Center at Houston, Houston, Texas 77030, United States, and [▽]Pain Therapy Service, Fondazione IRCCS Policlinico San Matteo, Pavia 27100, Italy. [⊗]These authors equally contributed to the manuscript.

ABSTRACT Tumor extracellular matrix (ECM) represents a major obstacle to the diffusion of therapeutics and drug delivery systems in cancer parenchyma. This biological barrier limits the efficacy of promising therapeutic approaches including the delivery of siRNA or agents intended for thermoablation. After extravasation due to the enhanced penetration and retention effect of tumor vasculature, typical nanotherapeutics are unable to reach the nonvascularized and anoxic regions deep within cancer parenchyma. Here, we developed a simple method to provide mesoporous silica nanoparticles (MSN) with a proteolytic surface. To this extent, we chose to conjugate MSN to Bromelain (Br—MSN), a crude enzymatic complex, purified from pineapple stems, that belongs to the peptidase papain family. This surface modification increased particle uptake in endothelial, macrophage, and cancer cell lines with minimal impact on cellular viability. Most importantly Br—MSN showed an increased ability to digest and diffuse in tumor ECM *in vitro* and *in vivo*.

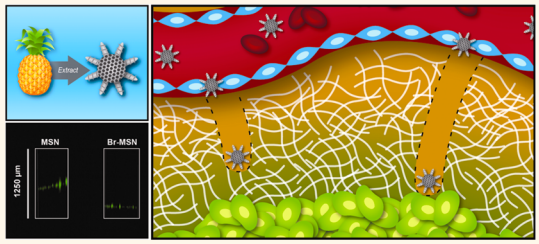

KEYWORDS: cancer · mesoporous silica nanoparticle modification · Bromelain · extracellular matrix digestion · cellular uptake

The ideal drug delivery platform for cancer therapy is designed to stably circulate through the bloodstream, target the tumor-associated vasculature, and extravasate in the subendothelial space.[1,2] Here, it is fundamental to achieve an efficient diffusion of the therapeutic payload in the interstitial space of the tumor[2] to maximize treatment efficiency. Due to their size and long circulation time, typical nanotherapeutics predominately base their targeting mechanism on exploiting the enhanced permeation and retention (EPR) effect that typically characterizes the tumor-associated vasculature.[3,4] However, beyond tumor vasculature, there are additional biological barriers[1,2,5] that are intrinsic to tumor parenchyma, which effectively hamper the diffusion of the carriers thus reducing their therapeutic efficacy. Tumor extracellular matrix (ECM), composed of proteoglycans, hyaluronic acid, collagen, elastin, laminin, and other structural proteins,[6] restricts the diffusion of drugs, macromolecular therapeutics and, to a greater extent, nanocarriers.[1,7−10] Previous reports indicate limited efficacy of promising curative approaches such as thermal ablation[7] or macromolecules like antibodies[8,9] but their delivery was hindered by the poor diffusion of the agents within the tumor parenchyma. Mathematical models and microfluidic systems were used to define nanotheraputic diffusion parameters within the tumor ECM,[10,11] suggesting that physical features such as size, shape and surface charge[10,12] can substantially affect the nanocarrier distribution within the ECM. Smart platforms designed to respond to tumor microenvironment features (*e.g.*, pH and high proteolytic activities)[2,13] or particles with unique material properties (*e.g.*, magnetic vectoring)[14] demonstrated successful navigation within tumor ECM through appropriate

* Address correspondence to etasciotti@houstonmethodist.org.

Received for review October 29, 2013 and accepted August 13, 2014.

Published online August 13, 2014
10.1021/nn502807n

surface functionalization. Considering that the ECM is highly susceptible to the action of proteases,[9,15,1613,18,19] we chose to develop a surface coating that bestows synthetic nanocarriers with proteolytic activity. For this purpose, we modified mesoporous silica nanoparticles (MSN) with Bromelain, a cocktail of cysteine and sulfhydryl proteases that belong to the papain family and are isolated from the stems of pineapples.[17,18] It contains a mixture of 9 different proteases[3,19] with distinct pH responsivenesses, enzymatic properties and molecular weights.[18,20,] Bromelain is weakly inhibited by the cysteine protease inhibitor E-64, and has been found to preferentially cleave the synthetic peptide sequence Bz-Arg-Arg-*p*-nitroanilide.[21] This extract is employed in the alimentary industry, where it is used to tenderize meat due to its ability to proficiently digest ECM.[22] Bromelain has previously received FDA approval for clinical use: in clinical practice, orally administered Bromelain is used for its anti-inflammatory[17,18,23] and anticoagulant properties.[17,24] The protein extract is currently used to ameliorate the symptoms of various diseases of inflammatory origin like osteoarthritis[25] and sinusitis.[26] Recently, these properties were shown to also be effective in inhibiting tumor growth and metastatic spread.[27,28] In this study, we show that the proteolytic activity of Bromelain can be transferred to the surface of MSN effectively enhancing their diffusion within the tumor ECM.

RESULTS AND DISCUSSION

MSN Physicochemical Properties. Transmission electron microscopy images indicated MSN displayed uniform size (50 nm) and spherical shape (Figure 1a,b). Pore size was estimated from the desorption branch using a standard BJH method (Barrett−Joyner−Halenda) and indicated an average pore size of 2.3 nm (Figure 1c). Surface area was measured through BET (Brunauer−Emmett−Teller) analysis showing a surface area to mass ratio of 650 m^2/g consistent with published reports.[29] The dye fluoresceine isothiocyanate (FITC) was incorporated into MSN during the synthesis (Figure 1d) in order to monitor the interactions with cells, and diffusion in matrigel and in tumor *in vivo*.

Bromelain Surface Modification. The surface functionalization of MSN with Bromelain (Br−MSN) was achieved through protein activation of the enzyme with EDC/sulfo-NHS prior to conjugation to (3-aminopropyl)-triethoxysilane (APTES)-modified MSN. Molecular bond signatures of Br−MSN were then evaluated through Fourier transform infrared spectroscopy (FTIR) (Figure 2a). APTES modified MSN displayed strong peaks at 1617 cm^{-1} representing the bending vibration of the aliphatic amine groups (N−H) and weak spectra between 2800 and 3000 cm^{-1} corresponding to aliphatic C−H stretching both characteristic of the APTES backbone.[30] The spectrum of pure Bromelain showed the

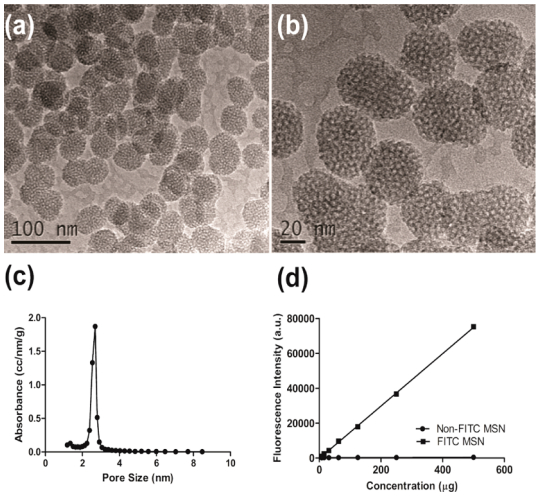

Figure 1. (a and b) TEM images of nonmodified MSN showing nonordered porosity. (c) Pore size distribution of nonmodified MSN analyzed using BJH; the most prominent pore size is 2.3 nm. (d) Fluorescent intensity comparison of FITC modified MSN and nonmodified MSN particles based on fluorescence spectroscopy.

presence of N−H stretching vibrations at 3338−3380 cm^{-1} in line with previous reports on Bromelain.[31] The C−N stretching vibration frequencies of Bromelain corresponded to the observed IR bands at 1517−1587, 1255−1290, and 1179−1149 cm^{-1}. In addition, the band at 1640−1700 cm^{-1} showed the presence of the characteristic C═O stretching groups of Bromelain.[31] FTIR spectra for Br−MSN exhibited peaks of both the N−H bending vibration of APTES at 1617 cm^{-1} and C−N stretching vibration of Bromelain at 1517−1587 cm^{-1} confirming surface functionalization of MSN. The passive absorption of Bromelain on nanoparticles has been considered as a control to assess proper surface modification and no residual protein after the standard washing steps was identified (Supporting Information Figure S1). To further validate bioconjugation to the surface of MSN, the ζ-potential was measured (Figure 2b) at each step of the procedure. The ζ-potential of FITC-modified MSN was slightly positive (+3.89 mV), and after APTES modification, this value further increased to +22.7 mV, as expected. Br−MSN yielded a drop in ζ-potential to −2.01 mV. This was likely due to Bromelain binding and absorption to the MSN surface as the ζ-potential of pure Bromelain was measured at −7.64 mV. Dynamic light scattering (DLS) analysis demonstrated a clear tendency of MSN to form small aggregates (173.71 nm) that slightly increased after Bromelain modification (213.62 nm) as shown in Figure 2c. The mass of Bromelain linked to the MSN surface was quantified with a Bradford protein assay, revealing 126 μg of protein extract/mg of unmodified particle was bound and absorbed (Figure 2d) after subtraction of the MSN background since the presence of APTES could react with the reagents of the kit. The ability of pure Bromelain to digest tumor

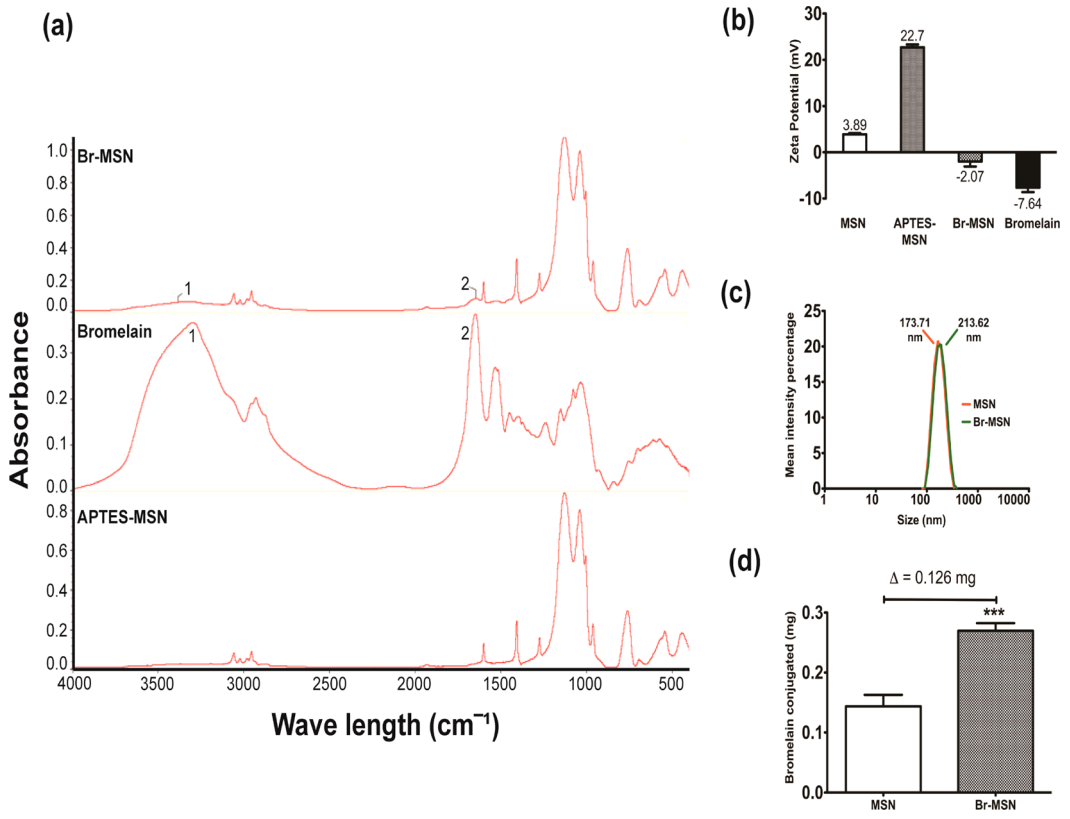

Figure 2. (a) Fourier transformed infrared spectroscopy spectrum of Br−MSN, pure Bromelain and APTES-MSN. Peaks 1 and 2 on the Br−MSN spectrum correspond to prominent peaks 1 and 2 of the pure Bromelain spectrum. (b) ζ-potential analysis of MSN, APTES-MSN, Br−MSN, and pure Bromelain. (c) Dynamic light scattering analysis of MSN (red) and Br−MSN (green). (d) Bromelain conjugation to MSN quantified *via* Bradford assay and analyzed using spectrophotometry. An equal amount of MSN was used as background.

ECM was investigated by embedding matrigel with FITC (0.75 mg/mL) before allowing it to polymerize. The matrigel was treated with increasing concentrations of Bromelain for 24 h and the release of the dye was analyzed through fluorimetric analysis on the digested supernatant. Bromelain increased the release of FITC in a dose dependent manner (Supporting Information Figure S2). In addition, we investigated the stability of Bromelain's proteolytic activity by storing a 10 mg/mL solution (PBS) for 24 h at 37 °C. The extract displayed significant autodigestive activities that affected its ability to digest matrigel (Supporting Information Figure S2). On the basis of these results, all experiments involving MSN were performed using freshly modified Br−MSN to preserve Bromelain activity.

Br−MSN Internalization and Impact on Cell Structure and Viability. Understanding the response of cells when interacting with a given drug delivery system is critical for determining its biocompatibility *in vitro*. Here, we studied the impact of Br−MSN treatment on three classes of cells relevant to tumor disease. Human umbilical vein endothelial cells (HUVEC), J774 macrophages, and MDA-MB-231 (MDA) breast cancer cells were treated with increasing concentrations of pure Bromelain, MSN, or Br−MSN. Cytotoxicity on all cell types was evaluated through WST-1 and Crystal Violet assays to measure cell viability as a function of metabolic activity and number of cells that remain adhered to the plate after treatments, respectively (Supporting Information Figure S3a and b). Both assays showed significant toxicity of pure Bromelain, in particular at the highest doses tested (1 and 10 ng/cell). However, the toxicity associated with Br−MSN was lower than free Bromelain, and MSN did not demonstrate any significant influence on cellular metabolic activity or attachment. Previous reports indicate that nanoparticle treatment can induce the activation of endolysosomal vesicles after cellular uptake.[32−34] This phenomenon was investigated with a Neutral Red assay (Supporting Information Figure S4), a test used to determine the modulation of endolysosomal activity by measuring the incorporation and retention of the Neutral Red dye within acidic intracellular vesicles.[35,36] MSN and Br−MSN increased Neutral Red uptake at all the tested doses in HUVEC, though the effect was not as pronounced for pure Bromelain treatment. No significant difference in Neutral Red uptake was detected after particle treatment in the other cell lines tested. Further investigation of the endolysosomal compartment in endothelial cells after treatment revealed that both MSN and Br−MSN increased the cytosolic ratio of the

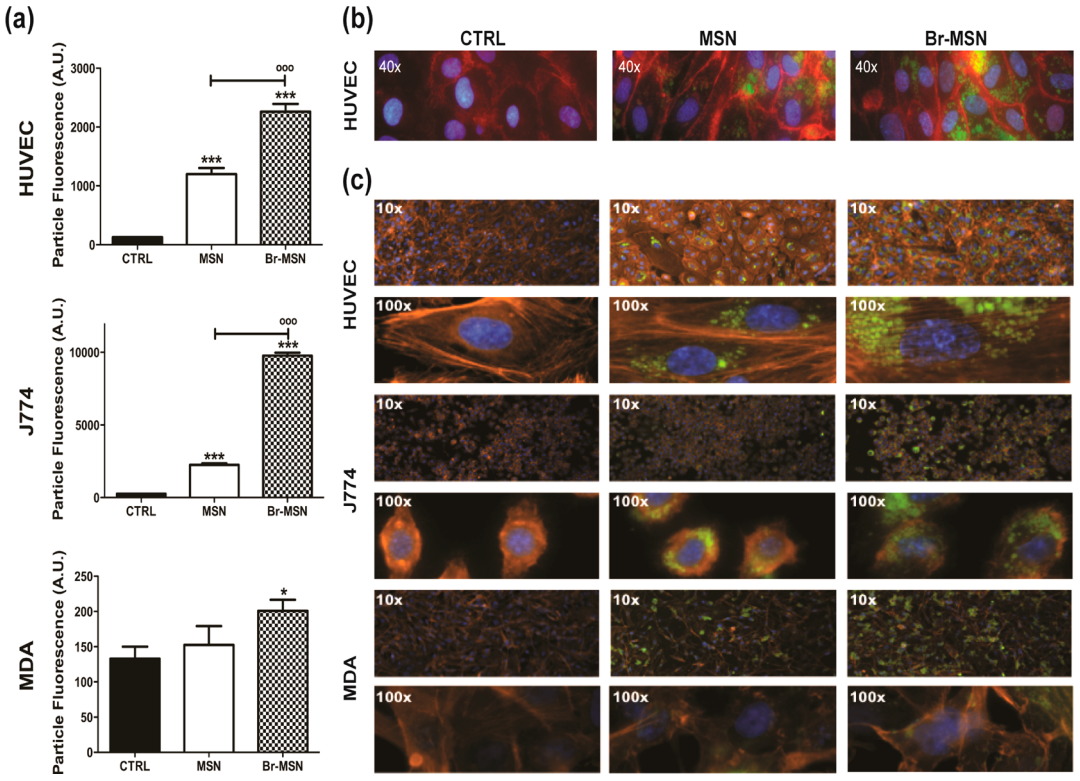

Figure 3. (a) Internalization of MSN and Br−MSN into MDA, J774 and HUVEC cell lines evaluated through FACS analysis. (b) Wide field epifluorescent micrographs of MSN and Br−MSN effects on intercellular endothelial junctions VE-cadherin (red). The particles are shown in green and the nuclei in blue. (c) Wide field epifluorescent micrographs of MSN and Br−MSN effects on cell actin (red) in HUVEC, J774 and MDA cells lines. The particles are shown in green and the nuclei in blue.

autophagocytosis proteins LC3II/LC3I (Supporting Information Figure S5a,b). These data suggest that particle internalization in HUVEC increased autophagocytosis, verifying the results of the Neutral Red assay and other reports.[32,34]

The internalization of MSN and Br−MSN was studied through flow cytometry after 24 h of treatment (Figure 3a). Bromelain surface modification increased nanoparticle uptake in all the cell lines tested (HUVEC, MDA, J774), and as expected, J774 macrophages and HUVEC, recognized as professional and nonprofessional phagocytic cells, respectively, internalized nanoparticles more efficiently than MDA. In all cell types, fluorescent micrographs showed that Br−MSN treated cells contained higher concentrations of nanoparticles compared to unmodified MSN, confirming previous data obtained with flow cytometry (Figure 3b,c). Increased affinity of Br−MSN for the cell membrane was also confirmed by SEM analysis performed after 15 min of treatment with different groups of particles (Supporting Information Figure S6). Furthermore, the impact of Br−MSN on cellular ultrastructure was evaluated by studying the VE-cadherin endothelial junctions and the actin cytoskeleton in all the cell lines tested through immunofluorescence microscopy. HUVEC were stained for VE-cadherin (red) and nuclei (blue), and treated with PBS, MSN (green), or Br−MSN (green) (Figure 3b). At a sublethal dose of 0.5 ng particles per cell, neither MSN nor Br−MSN affected endothelial intercellular junctions. F-actin staining confirmed the absence of any substantial impact of nanoparticle internalization on the cellular architecture (Figure 3c).

Br−MSN Ability To Adhere to Tumor ECM and Protelytic Properties. Flow chambers coated with matrigel were used to investigate Br−MSN and MSN adhesion to the matrix under physiological flow conditions (particles were dispersed in PBS at a concentration of 0.5 mg/mL, and passed throughout the chamber at a rate of 1 mL/min for 60 min). In the presence of flow, Br−MSN resulted in a 2-fold increase in particle accumulation compared to unmodified MSN (Figure 4a,b). The ability of Br−MSN to digest tumor ECM was assessed using matrigel and evaluated by following the release of an incorporated fluorescent dye (FITC) after treatment with the various classes of nanoparticles. At physiological pH (7.2) and temperature (37 °C), treatment with Br−MSN induced a 2-fold increase in the release of dye compared to control incubated just with PBS (Figure 4c) or with the same amount of MSN after 8 h. As previously reported in studies performed to evaluate Bromelain activity,[37] the proteolytic activity of Br−MSN was affected by decreasing the pH (Figure 4d), increasing the FBS concentration (Figure 4e) in the incubation solution, or decreasing the temperature (Figure 4f). However, in all tested conditions, Br−MSN consistently displayed

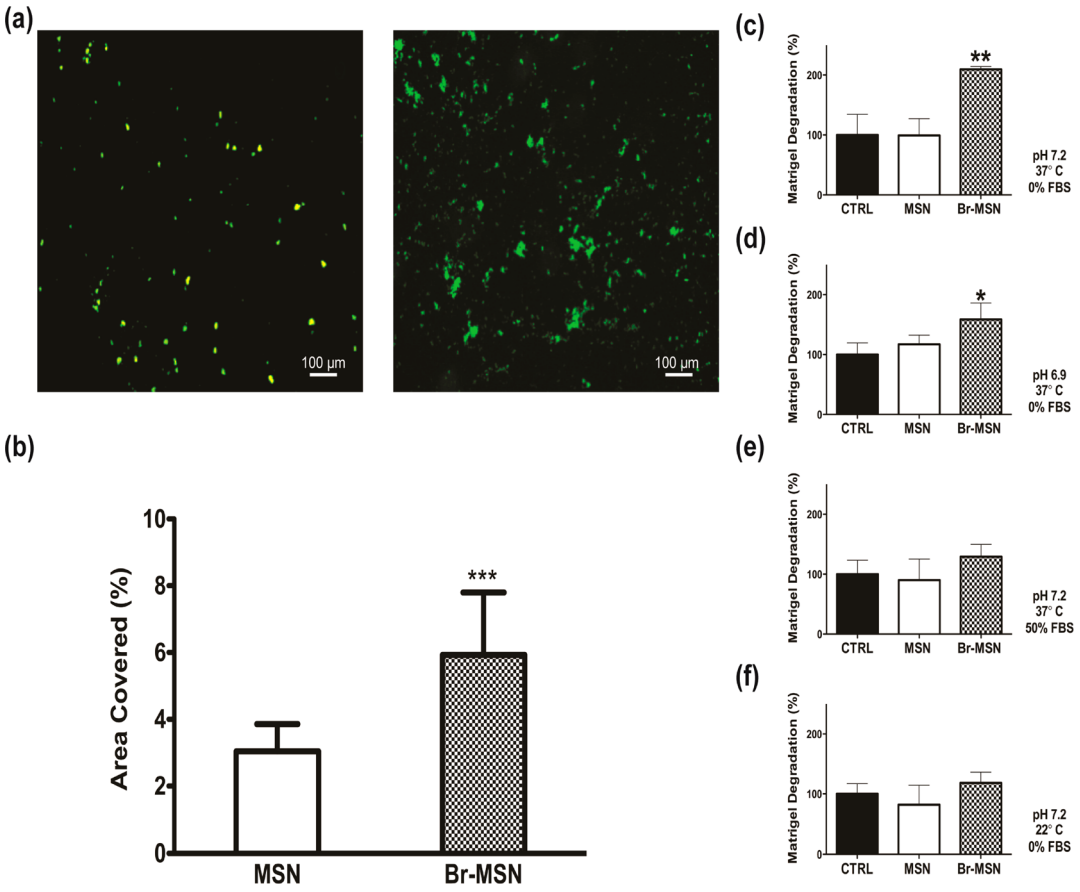

Figure 4. (a) MSN (left) and Br−MSN (right) adhesion on matrigel coated flow chambers after 1 h of flow in PBS; (b) quantification of MSN and Br−MSN covered area after flow; (c) matrigel digestion after 8 h of incubation with MSN and Br−MSN at pH 7.2, 37 °C, and 0% FBS; (d) matrigel digestion after 8 h of incubation with MSN and Br−MSN at pH 6.9, 37 °C, and 0% FBS; (e) matrigel digestion after 8 h of incubation with MSN and Br−MSN at pH 7.2, 37 °C, and 50% FBS; (f) matrigel digestion after 8 h of incubation with MSN and Br−MSN at pH 7.2, 22 °C, and 0% FBS.

superior enzymatic activity compared to control and MSN. In addition, similar experiments using polymerized gelatin as a substrate at physiological pH and temperature further validated the proteolytic surface activity of Br−MSN (Supporting Information Figure S7).

Br−MSN Affect Capillary Organization *in Vitro* and Diffuse in Tumor ECM. To further analyze the effect of Br−MSN on tumor ECM, we utilized the endothelial capillary network formation assay.[38] Matrigel's ability to induce endothelial cells to form capillary-like structures is well documented.[39] Figure 5a shows the organization of HUVEC stained with an MTT dye after 24 h of culture on matrigel. In the untreated or MSN pretreated matrigel, the formation of the expected capillary network was unhindered. However, cells seeded on the matrix pretreated with Br−MSN were not able to form the same multicellular organization, yet remained metabolically active. Quantification of the percentage of tubes formed in each treatment (Figure 5b), the covered area, total branching points, and total nets (Supporting Information Figure S8) confirmed the impairment on multicellular capillary organization exhibited by Br−MSN, likely due to its ability to degrade the matrigel substrate that the cells were plated upon. The level of particle diffusion in matrigel was determined after 24 h of incubation at 37 °C by collecting images along the *Z*-axis of a matrigel loaded well (Figure 5c). Br−MSN displayed a 2-fold increase in ECM penetration compared to unmodified MSN (Figure 5d). Lastly, we evaluated the ability of Br−MSN to diffuse within the tumor parenchyma *in vivo* using an orthotopic murine model of breast cancer (4T1 cells implanted in the mammary fat pad). Systemically injected Br−MSN (as well as naked MSN) did not accumulate at a tumor site in a concentration sufficient to perform an accurate analysis of tumor penetration (data not shown). As an *in vivo* proof of concept of Br−MSN proteolytic surface activity, we surgically exposed the tumors and locally injected MSN and Br−MSN at a depth of 700 μm into the tumor. The diffusion index of MSN and Br−MSN was evaluated at 1 and 24 h, acquired using intravital confocal microscopy (ICM) measuring the relative fluorescent intensity across a region of interest (ROI) composed of five concentric circles. After 1 h (Figure 5e and Supporting Information Videos 1 and 2), unmodified MSN were predominately

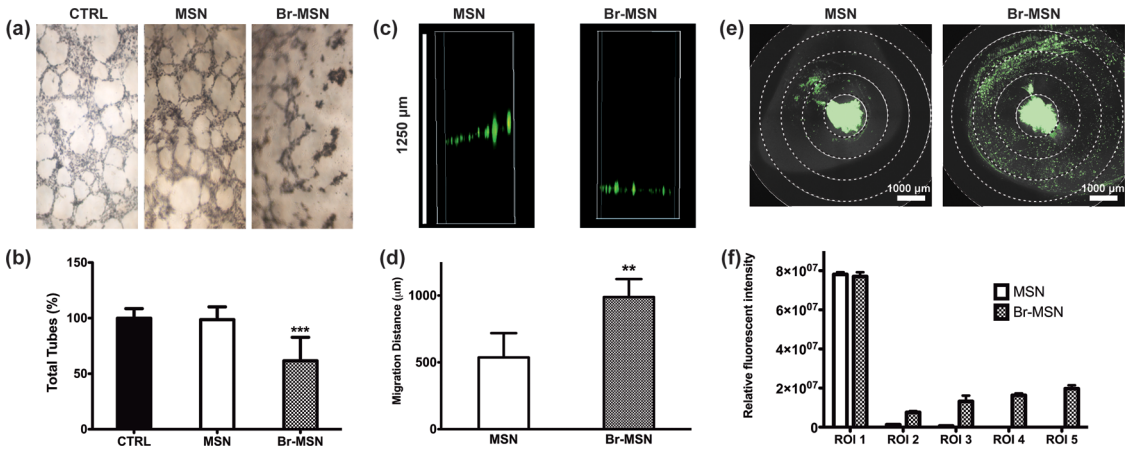

Figure 5. (a) Capillary tube formation of HUVEC seeded atop a layer of matrigel pretreated with PBS (CTRL), MSN and Br−MSN. Cell were stained with MTT. (b) Total amount of tubes formed in each experimental group. (c) Gravity driven migration of MSN and Br−MSN through a matrigel column. (d) quantification of the migration distance of the particles within the matrigel column. (e) Intravital microscopy images of tumors after 1 h following intratumoral injection of MSN and Br−MSN. (f) Relative fluorescent intensity measurements in the 5 exclusive circular ROI (region of interest) of selected Z-stacks.

localized at the site of injection (97.6%). In contrast, Br−MSN showed substantially higher diffusion throughout the tumor mass (42% of Br−MSN were dispersed across ROI 2−5). Twenty-four hours after injection (Supporting Information Figure S9), although most nanoparticles had been cleared from the tumor, unmodified particles still significantly remained in the injection site, while Br−MSN were found at the periphery of the field of view.

CONCLUSION

Tumor ECM significantly impairs the diffusion of the chemotherapeutics[40] impeding the adequate treatment of cancer cells that reside distantly from the blood vessels.[41] These limitations become even more pronounced when macromolecules[8,42,43] or nanoparticles[10,12] are used as therapeutics or delivery platforms. Typically, drug delivery systems designed to deeply penetrate the ECM are sensitive to the action of tumor extracellular metalloproteases that digest the deliverable's structure, favoring their diffusion in the interstitial space and the release of their payload.[2,44,45] On the other hand, an active approach designed to digest the tumor ECM by imparting carriers with hydrolytic activity could provide significant advantages for the delivery of therapeutics that must be protected during their route to the tumor cells (*e.g.*, siRNA and antibodies). Superior diffusion within the tumor parenchyma is also essential for therapeutics designed for thermal ablation[7] whose efficiency depends on their homogeneous distribution throughout the tumor volume. Herein, we describe a method of modifying the surface of a model nanotherapeutic (*i.e.*, MSN) with Bromelain to enhance their diffusion features upon contact with tumor ECM. Bromelain is an enzymatic complex extracted from pineapples, currently used for clinical purposes.[17,18,23−25] The addition of the proteolytic activity onto the surface of MSN was achieved by covalent attachment of the enzymatic complex using well established bioconjugation techniques. Br−MSN increased the affinity of the particles for tumor ECM, favored cell internalization, and showed a minor impact on cell viability and cell endolysosomal activity while avoiding any significant effect on endothelial junctions and cell cytoskeletal architecture. Br−MSN demonstrated efficient digestion and diffusion in matrigel, as well as inhibition of the organization of endothelial cells into tube-like structures when plated upon matrigel. Upon direct administration within the tumor, Br−MSN was observed to diffuse to a greater extent within 1 h than nonproteolytic MSN. Like most hydrolytic enzymes, the activity of Bromelain was hindered by environmental conditions, such as low pH, increased concentration of serum proteins, and decreased temperatures.[37] Thus, future endeavors aimed at developing therapeutic strategies based on this approach must implement features to enhance the circulation time and protect Bromelain surface modification during circulation. While further evaluation of the safety and immunogenicity of this approach must be conducted, we demonstrate that Bromelain surface modification represents a valuable approach to provide synthetic particles with proteolytic activity toward tumor ECM. Recent studies have demonstrated the use of controlled proteolytic activity on tumor parenchyma as a successful strategy to increase therapeutic efficacy of macromolecules,[8,9,11] as it favors the efficient diffusion of the treatment within the tumor parenchyma. However, the increase of proteolytic activity in cancer lesions is universally recognized as a hallmark of cancer progression and spreading. In this scenario, it is easy to

speculate that the proteolytic activity imparted to a particle designed for cancer treatment must be finely controlled. This aspect is extraordinarily important in terms of safety of the treatment, but in light of the results presented above, the presence of a transient proteolytic surface activity may be helpful to finely control particle diffusion within tumor parenchyma.

METHODS

Materials. The list of materials includes tetraethyl orthosilicate (TEOS), 3-(aminopropyl)triethoxysilane (APTES), hexadecyltrimethylammonium bromide (CTAB), fluorescein 5(6)-isothiocyanate (FITC), 2-propanol (IPA), ethanol, HCl, gelatin from porcine skin (gelatin), 2-mercaptoethanol (BME), and *N*-(3-diethylaminopropyl)-*N*′-ethylcarbodiimide hydrochloride (EDC) from Sigma-Aldrich (St. Louis, MO); 2-ethylsulfonic acid (MES), and NaCl from Acros Organics (Fairlawn, NJ); NH^4F and *N*-hydroxysulfosuccinimide (sulfo-NHS) from ThermoFisher Scientific (Waltham, MA); EHS sarcoma derived matrigel (matrigel) from Becton Dickinson and Company (Franklin Lakes, NJ); and hydroxylamine HCl from ICN Biomedicals (Aurora, OH).

Synthesis of Mesoporous Silica Nanoparticles. MSN were synthesized using a modified Stöber reaction. An amount of 162.909 mg of NH^4F and 144.87 mg of CTAB was dissolved in 48.24 mL of water. The solution was stirred vigorously at 80 °C for 1 h. Then, 0.988 mL of TEOS was added dropwise to the solution. The reaction proceeded for 2 h at 80 °C and was followed by two 50% ethanol washes, and then an overnight wash with 2% HCl by volume in ethanol to remove surfactants. The particles were finally washed with 50% ethanol and stored in IPA. FITC conjugated MSN were synthesized by co-condensing 0.075 mL of APTES and 4 mg of FITC with 0.92654 mL of TEOS.

APTES Surface Modification of Silica Nanoparticle Modification. Nanoparticles were modified with APTES by dispersing silica nanoparticles in a solution of 2% APTES and 5% Millipore water by volume in IPA at a concentration of 1 mg nanoparticle/mL APTES solution. The modification took place at 35 °C for 2 h under constant and vigorous agitation. After modification, the APTES modified nanoparticles were washed with IPA and stored in IPA at 4 °C until use.

Bromelain Conjugation to Silica Nanoparticles. Silica nanoparticles were conjugated to Bromelain *via* NHS/EDC chemistry. First, the protein was dissolved in a 0.1 M MES and 0.5 M NaCl activation buffer solution at a 1 mg/1 mL ratio. EDC and sulfo-NHS were added to the protein solution at 2 mM and 5 mM concentrations, respectively. The solution was allowed to react at room temperature for 15 min under constant agitation. After protein activation, BME was added at a concentration of 20 mM. APTES modified silica nanoparticles were dispersed in the reaction solution at a concentration of 1 mg of nanoparticle/3 mL reaction solution. The conjugation took place at room temperature for 2 h under constant and vigorous agitation. Hydroxylamine HCl was added to the solution at a concentration of 10 mM to quench the reaction. The Bromelain conjugated nanoparticles were then washed with PBS. The nanoparticles were used immediately after conjugation to control autodegradation of the Bromelain in aqueous solution.

Nanoparticle Characterization. Dynamic light scattering and ζ-potential characterization were performed using a Zetasizer ZEN3600 (Malvern, Worcestershire, U.K.). For DLS, scattered light detection was measure at 90° to the incident beam (a 25 mW laser at 660 nm wavelength). For ζ-potential analysis, the same parameters were used but scattered light was detected at 15°. Fourier transformed infrared spectroscopy was performed by creating a pellet of 5% sample and 95% KBr (Sigma-Aldrich) by volume and analyzing absorbance of the pellet on a Nicolet 6700 FT-IR Spectrometer (ThermoFisher Scientific). Samples were prepared for SEM by drying nanoparticles on a stage and sputter coating the sample with a 5 nm thick layer of platinum/palladium using a Sputter Coater 208HR (Cressington Scientific, Watford, U.K.). Microscopy images were taken using Nova NanoSEM 230 (FEI, Hillsboro, Oregon). TEM samples were prepared by drying nanoparticles onto 300 mesh carbon-coated copper grids. Samples were then sent to University of Texas at Austin for imaging by Dr. Tony Hu. BET and BJH analysis were utilized to analyze the surface area and porous structure of the MSN, deriving the isotherm analysis in the relative pressure range of 0.04−0.20.

Bromelain Conjugation to Silica Nanoparticles. To assess the amount of Bromelain conjugated to the surface of silica nanoparticles, a Bradford assay (Bio-Rad, Hercules, CA) was utilized. Analysis was performed using a DU 730 Life Science UV/Vis Spectrophotometer (Beckman Coulter, Indianapolis, IN) with absorbance at 595 nm.

Bromelain Autodigestive Effects and ECM Degradation. Autodigestive effects of Bromelain were tested by analyzing the level of matrigel degradation that preincubated Bromelain had in respects to fresh Bromelain. First, fluorescent matrigel was prepared by dispersing FITC into matrigel at a concentration of 0.75 mg/mL. The fluorescent matrigel was pipetted into 6 well plates and incubated at 37 °C for 2 h to promote gel formation. Bromelain was dispersed in PBS and allowed to incubate for 24 h prior to treatment for the preincubated Bromelain treatment. Treatment concentrations of fresh Bromelain and preincubated Bromelain ranged from 1×10^{-3} to 1.0 mg/mL PBS increasing by a factor of 10. After 24 h of incubation, the resultant degradation supernatant was collected for measurement and plate read *via* Synergy H4 Hybrid Reader (BioTek, Winooski, VT) at excitation/emission parameters 490 nm/525 nm.

Bromelain Conjugated Silica Nanoparticle Induced ECM Degradation. The efficacy of Br−MSN ECM degradation was analyzed by first adding fluorescent matrigel to a 12 well plate and then incubating the plate to promote gel formation. The wells were treated with PBS, 200 μg MSN in PBS, and 200 μg Br−MSN in PBS. After 8 h of incubation, the resultant degradation supernatant was collected for measurement and plate read *via* Synergy H4 Hybrid Reader (BioTek, Winooski, VT) at excitation/emission parameters 490 nm/525 nm. The same experiments were performed at pH 6.9, in the presence of 50% of FBS and at room temperature (22 °C)

Gelatin degradation efficacy was tested in a similar way using 5% gelatin mixed with FITC at a concentration of 0.75 mg FITC/mL of 5% gelatin solution instead of matrigel.

Bromelain Conjugated Silica Nanoparticle ECM Migration. The ability of silica nanoparticles conjugated to Bromelain to penetrate tumor ECM was analyzed by measuring the migration distance of fluorescent nanoparticles through a column of matrigel. Matrigel was pipeted into a 96 well plate and incubated. After gel formation, wells were treated with 100 μg of MSN dispersed in PBS, 100 μg of Br−MSN dispersed in PBS, and pure PBS as a control. The plate was incubated for 24 h and Z-stacks were obtained using a Nikon Eclipse Ti Inverted Fluorescent Microscope (Nikon Instruments, Inc., Melvillle, NY). The position of the fluorescent nanoparticle migration front was recorded and analyzed using NIS Elements AR software (Nikon Instruments, Inc.).

Br−MSN Activity Under Flow. Flow cell experimentation was performed by first adding matrigel to flow chambers and incubating them to promote gel formation. At room temperature, 0.5 mg of MSN in PBS, and 0.5 mg of Br−MSN in PBS were pumped through separate flow chambers at a rate of 1 mL/min. Chambers were washed with 1 mL of PBS after 1 h of flow to remove free fluorescent nanoparticles. The chambers were imaged using Nikon Eclipse Ti Inverted Fluorescent Microscope and the area of nanoparticle coverage for each image was measured using NIS Elements AR software.

Br−MSN Effect on Capillary Tube Formation. Endothelial capillary tube formation assays were performed by adding matrigel to a 96 well plate. The plate was incubated to allow for gel assembly. Wells were treated with 25 μg of Br−MSN in PBS, 25 μg MSN in PBS, a control of PBS, and incubated for 24 h. After incubation,

20 000 HUVEC cells/well were seeded and the plate was incubated for 15 h. Cells were stained with Trypan Blue Solution (Hyclone, Logan, UT) and imaged at 4× magnification *via* Nikon Eclipse TS 100 and Nikon Digital Sight (Nikon Instruments, Inc.). The images were sent to Ibidi LLC (Verona, WI) for analysis.

Cell Culture and Collection. All cells were obtained from American Type Culture Collection (Manassas, VA). MDA-MB-231 and J774 cells were cultured at 37 °C at 5% CO^2 atmospheric concentration in DMEM (Hyclone) enriched with 10% FBS, 1% penicillin and 1% L-glutamine. HUVEC PC-100-010 cells were cultured in enriched EBM-2 (Lonza, Walkersville, MD) at the same incubation parameters. MDA-MB-231 and HUVEC cells were lifted with trypsin while J774 cells were collected *via* scraping.

Cytotoxicity of Bromelain and Bromelain Conjugated Silica Nanoparticles. Cytotoxicity of Bromelain and silica nanoparticles conjugated to Bromelain was analyzed *via* WST-1 (Roche, Indianapolis, IN) and Crystal Violet (Sigma-Aldrich), while the evaluation of the endolysosomal compartment was achieved through Neutral Red Assay (Sigma-Aldrich). HUVEC, J774, and MDA-MB-231 cell lines were utilized. In total, 15 000 cells/well of each cell line were seeded into 96 well plates. Nanoparticles were dispersed in equal amounts of PBS and treatment groups were as follows: 0.1, 1, and 10 ng of pure Bromelain per cell; 0.1, 1, and 10 ng of MSN per cell; 0.1, 1, and 10 ng of Br−MSN per cell; as well as a control group of pure PBS. After 24 h of incubation, cell viability assays were performed and analyzed *via* plate absorbance reading.

Cell Treatment, Protein Extraction and Western Blotting Analysis. For the analysis of autophagy biomarker LC3II/LC3I, 3×10^5 cells (MDA, HUVEC and J774) were seeded into a 6 well plate. After 24 h, each cell line was treated with the same amount (1 ng/cell) of MSN and Br−MSN for 24 h. Nontreated cells were used as controls. Cells were lysed and proteins were extracted using RIPA buffer (Thermo) with protease inhibitor cocktail (Thermo) and PMSF at 0.5 mM.

Twenty micrograms of whole cell lysate was loaded onto a 12% SDS polyacrylamide gel and then transferred on a PVDF membrane for Western blotting analysis. The membranes were blocked in 5% nonfat milk in TTBS for 2 h and then incubated overnight at 4 °C with rabbit anti-LC3 (Novus Biologicals; 1:2000) and mouse anti-GAPDH (Santa Cruz Technologies; 1:200) primary antibodies. Then membranes were incubated with HRP (horseradish peroxidase)-conjugated anti-rabbit and anti-mouse IgG (Sigma−Aldrich) secondary antibodies, respectively. The bands were detected by chemiluminescence using the SuperSignal West Dura Chemiluminescent Substrate (Thermo); images were visualized, acquired and analyzed with ChemiDoc XRS+ System and Image Lab software (Bio-Rad).

Bromelain Conjugated Silica Nanoparticle Cellular Internalization. To test the internalization of nanoparticles into HUVEC, J774, MDA-MB-231 cell lines, flow cytometry was utilized. In total, 200 000 cells/well of each cell line were seeded separately into a 6 well plate. Nanoparticles used for treatment were dispersed in an equal amount of PBS as used in control experiments. Treatment groups consisted of MSN, Br−MSN, and a control of pure PBS. Cells were treated with 1 ng of particle per cell as well as pure PBS. Flow cytometry analysis was performed after 24 h incubation with an LSR Fortessa Special Order Research Product (Becton Dickinson). At least 20 000 counts were obtained for each sample for statistical significance.

SEM was also used to investigate nanoparticle internalization for each cell line. For this, 50 000 cells/well of each cell line were seeded into a 4 chambered imaging slide. Treatment groups consisted of MSN, Br−MSN, and a control of pure PBS. Cells were treated with 1.5 ng particle per cell. Fixation was performed after 15 min, sputter coated and imaged.

Fluorescent microscope samples were prepared on imaging slides, and 50 000 cells/well of each cell line were seeded into a 4 chambered imaging slide. Cells were treated with 1 ng of MSN/cell, 1 ng Br−MSN/cell, and pure PBS. After 24 h of incubation, the cells were fixed, stained for actin with Alexa Fluor 555 Phalloidin (Life Technologies, Grand Island, NY), and nuclear stained with Molecular Probes DAPI/Prolong Gold (Life Technologies). Similar techniques were used to evaluate the effect of particles on endothelial VE-cadherin. Slides were imaged using Nikon Eclipse Ti Inverted Fluorescent Microscope and analyzed *via* NIS Elements AR.

Animal Care. Six to eight week old female BALB/c mice were purchased from Charles River Laboratories. Mice were housed under standard 12 h light−dark cycles and fed *ad libitum*. All animal protocols were according to the Guide for the Care and Use of Laboratory Animals and approved by the Animal Care and Use Committee at Houston Methodist Research Institute.

Intravital Confocal Microscopy. A total of 1×10^4 of 4T1 cells, suspended in 100 μL of RPMI 1640 (ATCC) supplemented with 10% heat inactivated FBS, were injected into the left rear flank of female BALB/c mice. Calipers were used to measure tumor diameters. Tumor volume was calculated using the following formula: [Length × (width)^2]/2. On day 10, when the tumor volume reached 100 mm^3, the mice were randomly assigned to two groups ($n = 3$). Groups were treated *via* intratumor administration with either FITC labeled MSN or Br−MSN at 12.5 μg of nanoparticles in 5 μL of PBS. Mice were maintained anesthetized by inhalation of 2% isoflurane throughout the experiment. Under deep anesthesia, tumors were exposed with surgical dissection of the skin while an intact blood supply was maintained. The nanoparticle treatment was injected directly inside the tumor using a Hamilton Neuros Syringe. The needle sleeve of the Neuros syringe was adjusted to allow a needle exposure of 700 μm to achieve a superficial injection of MSN inside the tumor. After 60 min, images were acquired from 200 μm Z-stacks by intravital confocal microscopy (ICM) using an upright Nikon A1R laser scanning confocal microscope equipped with a resonance scanner, motorized and heated stage. Stitching was used to reconstruct a large image from 4 (2 × 2) block images for each Z-stack. All settings including laser power, gain, offset, and pinhole diameter were maintained the same throughout each acquisitions. The skin flap was closed with 5−0 nylon sutures after imaging. After 24 h, the tumors were imaged again for MSN distribution as described earlier. All images were analyzed with NIS-Elements AR 4.12.01 64-bit software. The Z-stack with the highest fluorescent intensity was used for further analysis. Threshold was defined in a manner to eliminate autofluorescence and the same threshold was applied for all image analysis. The relative fluorescent intensity was measured using a ROI (region of interest) constructed using five concentric circles in the selected Z-stacks.

Statistical Analysis. All the numeric data are the result of a minimum of three independent experiments. Statistical computation was performed with Prism GraphPad software. The statistical significance was calculated using a one-way Anova method, followed by Dunnett's test or with two-tailed unpaired Student's *t* test.

Conflict of Interest: The authors declare no competing financial interest.

Supporting Information Available: FTIR spectrum of Bromelain passively absorbed on MSN; matrigel degradation upon subjection to different concentrations of Bromelain; cell viability results for MDA, J774 and HUVE cells after treatment with pure Bromelain, MSN, and Br−MSN; evaluation of endolysosomal activity in MDA, J774, and HUVEC; Western blot analysis and densitometric measurements of LC3-I and LC3-II in MDA, HUVEC, and J774 cells; SEM of immediate cellular effects of Br-MSN on HUVEC, J774, and MDA cell lines; analysis of covered area, branching points, and total nets formed by HUVECs seeded on a matrigel bed; analysis of diffusion index of MSN and Br−MSN in tumors. Videos of Intravital confocal microscopic images of tumors with 3D reconstruction at 1 h following intratumoral injection of Bromelain modified MSN (Movie 1.avi) and MSN (Movie 2.avi). This material is available free of charge *via* the Internet at http://pubs.acs.org.

Acknowledgment. The authors acknowledge support from the Alliance for NanoHealth Department of Defense Telemedicine & Advanced Technology Research Center (W81XWH-10-2-0125 and W81XWH-09-2-0139), the National Institutes for Health (1R21CA173579-01A1), the Department of Defense/Breast Cancer Research Program (W81XWH-12-10414).

This study was partially supported by Italian Ministry of Health RF-2010-2318372 (to F.T.), Bianca Garavaglia Association, Busto Arsizio, Va, Italy, NIH predoctoral fellowship 1F31CA154119. A kind acknowledgment to D. Bravo for his intellectual contribution, M. Landry for graphical assistance, Enrica De Rosa for performing the intravital imaging experiments and for helping with data acquisition and Ashley Torregrossa for her contribution to the finalization of the manuscript. Manuscript in memory of Katelyn Dallas Bravo (02/28/1999–06/17/2010).

REFERENCES AND NOTES

1. Rakesh, K. J.; Triantafyllos, S. Delivering Nanomedicine to Solid Tumors. *Nat. Rev. Clin. Oncol.* **2010**, *7*, 653–664.
2. Wong, C.; Stylianopoulos, T.; Cui, J.; Martin, J.; Chauhan, V. P.; Jiang, W.; Popović, Z.; Jain, R. K.; Bawendi, M. G.; Fukumura, D. Multistage Nanoparticle Delivery System for Deep Penetration into Tumor Tissue. *Proc. Natl. Acad. Sci. U.S.A.* **2011**, *108*, 2426–2431.
3. Wang, A. Z.; Langer, R.; Farokhzad, O. C. Nanoparticle Delivery of Cancer Drugs. *Ann. Rev. Med.* **2012**, *63*, 185–198.
4. Shekhar, C. Lean and Mean: Nanoparticle-Based Delivery Improves Performance of Cancer Drugs. *Chem. Biol.* **2009**, *16*, 349–350.
5. Torchilin, V. Tumor Delivery of Macromolecular Drugs Based on the Epr Effect. *Adv. Drug Delivery Rev.* **2011**, *63*, 131–135.
6. Plopper, G. *The Extracellular Matrix and Cellular Adhesion, in Cells*; Lewin, B. C., Cassimens, L.; Lingappa, V. R.; Plopper, G., Eds.; Jones and Bartlett: Sudbury, MA, 2007.
7. Hirsch, L. R.; Stafford, R.; Bankson, J.; Sershen, S.; Rivera, B.; Price, R.; Hazle, J.; Halas, N.; West, J. Nanoshell-Mediated near-Infrared Thermal Therapy of Tumors under Magnetic Resonance Guidance. *Proc. Natl. Acad. Sci. U.S.A.* **2003**, *100*, 13549–13554.
8. Beyer, I.; Li, Z.; Persson, J.; Liu, Y.; van Rensburg, R.; Yumul, R.; Zhang, X. B.; Hung, M. C.; Lieber, A. Controlled Extracellular Matrix Degradation in Breast Cancer Tumors Improves Therapy by Trastuzumab. *Mol. Ther.* **2011**, *19*, 479–489.
9. Eikenes, L.; Bruland, Ø. S.; Brekken, C.; de Lange Davies, C. Collagenase Increases the Transcapillary Pressure Gradient and Improves the Uptake and Distribution of Monoclonal Antibodies in Human Osteosarcoma Xenografts. *Cancer Res.* **2004**, *64*, 4768–4773.
10. Stylianopoulos, T.; Poh, M.-Z.; Insin, N.; Bawendi, M. G.; Fukumura, D.; Munn, L. L.; Jain, R. K. Diffusion of Particles in the Extracellular Matrix: The Effect of Repulsive Electrostatic Interactions. *Biophys. J.* **2010**, *99*, 1342–1349.
11. Netti, P. A.; Berk, D. A.; Swartz, M. A.; Grodzinsky, A. J.; Jain, R. K. Role of Extracellular Matrix Assembly in Interstitial Transport in Solid Tumors. *Cancer Res.* **2000**, *60*, 2497–2503.
12. Mitragotri, S.; Lahann, J. Materials for Drug Delivery: Innovative Solutions to Address Complex Biological Hurdles. *Adv. Mater.* **2012**, *24*, 3717–3723.
13. Gullotti, E.; Yeo, Y. Extracellularly Activated Nanocarriers: A New Paradigm of Tumor Targeted Drug Delivery. *Mol. Pharmaceutics* **2009**, *6*, 1041–1051.
14. Kong, S. D.; Zhang, W.; Lee, J. H.; Brammer, K.; Lal, R.; Karin, M.; Jin, S. Magnetically Vectored Nanocapsules for Tumor Penetration and Remotely Switchable on-Demand Drug Release. *Nano Lett.* **2010**, *10*, 5088–5092.
15. Eikenes, L.; Tari, M.; Tufto, I.; Bruland, Ø. S.; de Lange Davies, C. Hyaluronidase Induces a Transcapillary Pressure Gradient and Improves the Distribution and Uptake of Liposomal Doxorubicin (Caelyx) in Human Osteosarcoma Xenografts. *Br. J. Cancer* **2005**, *93*, 81–88.
16. Ganesh, S.; Gonzalez-Edick, M.; Gibbons, D.; Van Roey, M.; Jooss, K. Intratumoral Coadministration of Hyaluronidase Enzyme and Oncolytic Adenoviruses Enhances Virus Potency in Metastatic Tumor Models. *Clin. Cancer Res.* **2008**, *14*, 3933–3941.
17. Maurer, H. Bromelain: Biochemistry, Pharmacology and Medical Use. *CMLS, Cell. Mol. Life Sci.* **2001**, *58*, 1234–1245.
18. Pavan, R.; Jain, S.; Shraddha; Kumar, A. Properties and Therapeutic Application of Bromelain: A Review. *Biotechnol. Res. Int.* **2012**, *2012*, No. 976203.
19. El-Gharbawi, M.; Whitaker, J. R. Fractionation and Partial Characterization of the Proteolytic Enzymes of Stem Bromelain. *Biochemistry* **1963**, *2*, 476–481.
20. Harrach, T.; Eckert, K.; Schulze-Forster, K.; Nuck, R.; Grunow, D.; Maurer, H. R. Isolation and Partial Characterization of Basic Proteinases from Stem Bromelain. *J. Protein Chem.* **1995**, *14*, 41–52.
21. Lee, K. L.; Albee, K. L.; Bernasconi, R. J.; Edmunds, T. Complete Amino Acid Sequence of Ananain and a Comparison with Stem Bromelain and Other Plant Cysteine Proteases. *Biochem. J.* **1997**, *327* (Pt. 1), 199–202.
22. Istrati, D.; Vizireanu, C.; Dima, F.; Dinică, R. Effect of Marination with Proteolytic Enzymes on Quality of Beef Muscle. *St. Cerc. St. CICBIA* **2012**, *13*, 81–89.
23. Tochi, B. N.; Wang, Z.; Xu, S.-Y.; Zhang, W. Therapeutic Application of Pineapple Protease (Bromelain): A Review. *Pak. J. Nutr.* **2008**, *7*, 513–520.
24. Heinicke, R.; van der Wal, L.; Yokoyama, M. Effect of Bromelain (Ananase) on Human Platelet Aggregation. *Cell. Mol. Life Sci.* **1972**, *28*, 844–845.
25. Brien, S.; Lewith, G.; Walker, A.; Hicks, S. M.; Middleton, D. Bromelain as a Treatment for Osteoarthritis: A Review of Clinical Studies. *J. Evidence-Based Complementary Altern. Med.* **2004**, *1*, 251–257.
26. Braun, J.; Schneider, B.; Beuth, H. Therapeutic Use, Efficiency and Safety of the Proteolytic Pineapple Enzyme Bromelain-Pos in Children with Acute Sinusitis in Germany. *In Vivo* **2005**, *19*, 417–421.
27. Batkin, S.; Taussig, S.; Szekerezes, J. Antimetastatic Effect of Bromelain with or without Its Proteolytic and Anticoagulant Activity. *J. Cancer Res. Clin. Oncol.* **1988**, *114*, 507–508.
28. Chobotova, K.; Vernallis, A. B.; Majid, F. A. A. Bromelain's Activity and Potential as an Anti-Cancer Agent: Current Evidence and Perspectives. *Cancer Lett.* **2010**, *290*, 148–156.
29. Chiang, Y.-D.; Lian, H.-Y.; Leo, S.-Y.; Wang, S.-G.; Yamauchi, Y.; Wu, K. C.-W. Controlling Particle Size and Structural Properties of Mesoporous Silica Nanoparticles Using the Taguchi Method. *J. Phys. Chem. C* **2011**, *115*, 13158–13165.
30. Maria Chong, A.; Zhao, X. Functionalization of Sba-15 with Aptes and Characterization of Functionalized Materials. *J. Phys. Chem. B* **2003**, *107*, 12650–12657.
31. Soares, P. A.; Vaz, A. F.; Correia, M. T.; Pessoa, A., Jr.; Carneiro-da-Cunha, M. G. Purification of Bromelain from Pineapple Wastes by Ethanol Precipitation. *Sep. Purif. Technol.* **2012**, *98*, 389–395.
32. Blanka, H. K.; Catherine, C. B.; Seher, G.-A.; Lucienne, J.-J. Induction of Oxidative Stress, Lysosome Activation and Autophagy by Nanoparticles in Human Brain-Derived Endothelial Cells. *Biochem. J.* **2012**, *441*, 813–821.
33. Wu, S.; Li, Z.; Han, J.; Han, S. Dual Colored Mesoporous Silica Nanoparticles with Ph Activable Rhodamine-Lactam for Ratiometric Sensing of Lysosomal Acidity. *Chem. Commun.* **2011**, *47*, 11276–11278.
34. Stern, S. T.; Adiseshaiah, P. P.; Crist, R. M. Autophagy and Lysosomal Dysfunction as Emerging Mechanisms of Nanomaterial Toxicity. *Part. Fibre Toxicol.* **2012**, *9*, 20.
35. Albini, A.; Mussi, V.; Parodi, A.; Ventura, A.; Principi, E.; Tegami, S.; Rocchia, M.; Francheschi, E.; Sogno, I.; Cammarota, R. Interactions of Single-Wall Carbon Nanotubes with Endothelial Cells. *Nanomedicine (N. Y., NY, U.S.)* **2010**, *6*, 277–288.
36. Monteiro-Riviere, N. A.; Inman, A. O.; Zhang, L. Limitations and Relative Utility of Screening Assays to Assess Engineered Nanoparticle Toxicity in a Human Cell Line. *Toxicol. Appl. Pharmacol.* **2009**, *234*, 222–235.
37. Khan, R. H.; Rasheedi, S.; Haq, S. K. Effect of pH, Temperature and Alcohols on the Stability of Glycosylated and Deglycosylated Stem Bromelain. *J. Biosci.* **2003**, *28*, 709–714.

38. Donovan, D.; Brown, N.; Bishop, E.; Lewis, C. Comparison of Three *in Vitro* Human 'Angiogenesis' Assays with Capillaries Formed *in Vivo*. *Angiogenesis* **2001**, *4*, 113–121.
39. Ponce, M. L. *In Vitro* Matrigel Angiogenesis Assays. In *Angiogenesis Protocols*; Murray, J. C., Ed.; Humana Press: Totowa, NJ, 2001; pp 205−209.
40. Cukierman, E.; Khan, D. R. The Benefits and Challenges Associated with the Use of Drug Delivery Systems in Cancer Therapy. *Biochem. Pharmacol.* **2010**, *80*, 762–770.
41. Primeau, A. J.; Rendon, A.; Hedley, D.; Lilge, L.; Tannock, I. F. The Distribution of the Anticancer Drug Doxorubicin in Relation to Blood Vessels in Solid Tumors. *Clin. Cancer Res.* **2005**, *11*, 8782–8788.
42. Choi, I.-K.; Strauss, R.; Richter, M.; Yun, C.-O.; Lieber, A. Strategies to Increase Drug Penetration in Solid Tumors. *Front. Oncol.* **2013**, *3*, 193.
43. Minchinton, A. I.; Tannock, I. F. Drug Penetration in Solid Tumours. *Nat. Rev. Cancer* **2006**, *6*, 583–592.
44. Chau, Y.; Padera, R. F.; Dang, N. M.; Langer, R. Antitumor Efficacy of a Novel Polymer−Peptide−Drug Conjugate in Human Tumor Xenograft Models. *Int. J. Cancer* **2006**, *118*, 1519–1526.
45. Chau, Y.; Dang, N. M.; Tan, F. E.; Langer, R. Investigation of Targeting Mechanism of New Dextran-Peptide-Methotrexate Conjugates Using Biodistribution Study in Matrix-Metalloproteinase-Overexpressing Tumor Xenograft Model. *J. Pharm. Sci.* **2006**, *95*, 542–551.